Chemical Engineering Journal 429 (2022) 132159

Contents lists available at ScienceDirect

Chemical Engineering Journal

journal homepage: www.elsevier.com/locate/cej

Gecko-inspired ultrasensitive multifunctional mechano-optical smart membranes

Yang Liu [a], Shaoxin Song [b], Meng Liu [b], Yue Hu [c], Lu-wen Zhang [c], Hyunsik Yoon [d], Lili Yang [b,*], Dengteng Ge [a,*]

[a] State Key Laboratory for Modification of Chemical Fibers and Polymer Materials, Institute of Functional Materials, Donghua University, Shanghai 201620, China
[b] State Key Laboratory for Modification of Chemical Fibers and Polymer Materials, College of Materials Science and Engineering, Donghua University, Shanghai 201620, China
[c] Department of Engineering Mechanics, School of Naval Architecture, Ocean and Civil Engineering, Shanghai Jiao Tong University, Shanghai 200240, China
[d] Department of Chemical and Biomolecular Engineering, Seoul National University of Science & Technology, Seoul 01811, Korea

ARTICLE INFO

Keywords:
Mechano-optical material
Gecko-inspired
Ultrasensitivity
Multifunction

ABSTRACT

Mechano-optical materials are of great importance in smart window, security, display and camouflages. However, fabricating ultrasensitive optical devices with wide range still remains great challenging. Inspired from the fast tail amputation of gecko utilizing weak non-ossificated septum, herein, we report an ultrasensitive mechano-optical membrane based on weak dye layer between silica nanoparticles and soft polydimethylsiloxane matrix. Owing to the light scattering from dye-induced internal cavitation, the transmittance dramatically decreases by ~44% at initial small strain level (15%) and a high sensitivity ($S > 2$) is kept within an abroad strain range (0 ~ 35%). Moreover, a high total transmittance tuning range of ~75% is exhibited. Simulation and experimental monitoring demonstrate the effective weakening of interface energy. The potential applications in smart window, sensor, anti-counterfeiting also exhibit the multifunctionality of our smart membranes. This facile and low-cost approach enables the large-scale production and applications of mechano-optical membranes and this interface design provides a general way to develop ultrasensitive mechano-responsive materials.

1. Introduction

Mechano-responsive smart materials have gained great attention due to their switchable optical, electrical or wettability performance via deformation under external stimuli such as force, heat, light, moisture, solvent [1–3]. For example, mechano-optical materials exhibit switchable light transmittance properties, making them attractive for potential applications in energy-efficient architectural/vehicular windows, sensors, camouflages and bendable medical devices. Compared with traditional switching optical materials via reversible arrangement of particles [4] or liquid crystals [5–7] through electric field, oxidation–reduction reaction of chromogenic materials [8–11] or phase transition under heat/light activation [12,13], mechano-optical materials have advantages because they offer a simple, low-cost, stable approach and allow for independent control. In general, mechano-optical materials are conventionally achieved by tunable light scattering or transmittance of patterned surfaces, e.g. nanopillars on wavy elastomer [14], tilted pillars on wrinkled Polydimethylsiloxane (PDMS) [15–17], shape memory elastomer with microprism or microlens arrays [18,19], and self-similar hierarchical wrinkles [20]. Despite the advantages in stability and fabrication, these methods still suffer from mild sensitivity or moderate transmittance modulation range upon stretching, which seriously restrict the practical applications.

To improve the optical tunablity, Prof. Sun utilized the opening of longitudinal/ transverse microscale cracks of rigid layer on soft substrate when stretched and exhibited a great transparency change of ~ 28% at the beginning small strain of 10% [21,22]. The change rate then slowed down basically due to the limited expansion of cracks. A higher transmittance range up to 76% is shown via one-sided surface wrinkling-cracking patterns induced by stretching UV/Ozone-treated PDMS when applied strain increases to 50% [23]. Excellent optical tunability has been displayed via the opening of surface patterns, however, this membrane only displays high mechano-optical sensitivity within beginning small strain. Furthermore, the micro/nano-scale surface features are fragile to external mechanical loading, dust or moisture, while an extra protective layer is required which accordingly increases the

* Corresponding authors.
E-mail addresses: liliyang@dhu.edu.cn (L. Yang), dengteng@dhu.edu.cn (D. Ge).

https://doi.org/10.1016/j.cej.2021.132159
Received 27 June 2021; Received in revised form 17 August 2021; Accepted 29 August 2021
Available online 4 September 2021

device complexity and cost. Therefore, it will be highly desired to achieve high-sensitive, robust tunable optical device from integrated materials via facile, low-cost approaches. Inspired by chameleon or squids which switch the body color by enlarging the chromophores embedded in the skins, our group and collaborators previously reported a robust, mechano-optical membrane of silica Nanoparticles (NPs) embedded in bulk elastomeric PDMS based on the diffusion light scattering and absorption from internal cavitation [24,25]. Although a high up to 70% of optical transmittance can be tuned, however, the mechano-optical sensitivity remains to be improved [26].

Constructing fast-responsive interfaces for generating/vanishment of scattering under strain may be a preferential alternative. Actually in nature, many organisms utilize weak-boundary layer to achieve quick response to external attack, temperature change or self-growth. As illustrated in Fig. 1A, gecko makes fast tail amputation via a weak non-ossificated septum in one caudal vertebrae for avoiding attack [27]. The molting of arthropods is involving molting hormone-mediated mineral or enzyme or protein change between the new and old shell [28]. Inspired by this mechanism, herein, an ultrasensitive tunable optical membrane via dye-induced weak-boundary layer is reported. Based on this interface design, the transmittance could be dramatically reduced by ~44% at the beginning strain $\leq$ 15%, resulting from weak-boundary layer-enhanced formation of cavitation. This membrane exhibits a high total transmittance tuning range of ~75% and can be reversibly tuned for 2000 cycles without losing structural integrity and optical performance. Our approach provides a facile way for robust, highly sensitive mechano-optical device.

2. Experimental details

2.1. Materials

Ammonium hydroxide (~28–30%) and ethanol (99%, GreaGent, Shanghai, China) were purchased from GreaGent, Shanghai, China. Tetraethyl orthosilicate (TEOS, 98%, Sinopharm Chemical Reagent Co., Ltd, Shanghai, China), isopropanol (IPA, 99.8%, Macklin, Shanghai, China), PDMS (Sylgard-184, Dow Corning, Midland, MI, USA), Sudan II (99%, Adamas, Basel, Switzerland), Alizarin Cyanin Green F(AR, Aladdin, Shanghai, China) and Disperse Blue E-4R(97%, Shanghai yuanye Bio-Technology Co., Ltd, Shanghai, China) were used as received.

2.2. Fabrication of ultrasensitive smart membrane

Silica NPs were synthesized by the Stöber method [29]. SiO_2 NPs were dispersed into IPA with concentration of 10 wt% and ultrasonicated for 2 h to prepare the first spray solution. Secondly, dye(D) (Disperse Blue E-4R) was dissolved in acetone or dye(S) (Sudan II) was dissolved in IPA at a concentration of 1 mg ml^{-1}. NPs/IPA solution was sprayed 4 times and then dye solution was sprayed on the polystyrene (PS) Petri dish at a distance of 5 cm and a moving speed of ~ 5 cm s^{-1}. Dow Corning Sylgard 184 and its curing agent were mixed at a weight ratio 10:1. After degassing, PDMS precursor was cast on the sprayed Petri dish and then cured at 65 °C for 4 h. Finally, the hybrid membrane was carefully peeled from the Petri dish.

2.3. Fabrication of colored ultrasensitive smart membrane

The dye dispersed PDMS layer was prepared by ultrasonic mixing of 15 g of liquid PDMS (Sylgard 184), 0.07 wt% of dye (Sudan II, Disperse blue E-4R or Alizarin Cyanin Green F), 10 ml of ethanol and 15 ml of toluene for 8 h. The mixture was dried in a vacuum oven at 80 °C for 8 h to completely remove ethanol and toluene. Then, 1.5 g of curing agent was added. After stirring and degassing, the mixture was poured into sprayed NPs-dye coating on Petri dish and then cured at 65 °C for 4 h. Finally, the hybrid membrane was peeled off the substrate.

2.4. Characterization

The surface morphologies of the samples were examined using a field-emission scanning electron microscope (S-4800, Hitachi, Japan). The scattering spectra at various strains and the cycle-dependent transmittance were collected from a USB2000 fiber optical spectrometer (Ocean Optics, USA) combined with a custom-built stretcher. The peeling force of dye@glass/PDMS was measured using an electronic universal testing machine (RWT10, Reger, China), and the details were seen in supporting information. XRD images were taken by X-ray Diffraction (D2 Phaser, Bruker, Germany). Microscope images were taken by optical microscopy (BX 63, Olympus, Japan) in transmission modes. Digital photos were collected using a digital camera (Nikon 1 J5, Japan). Thermogravimetric analysis (TG) was obtained by thermogravimetric analyzer (TG 209 F1, Netzsch, Germany).

3. Results and discussion

3.1. Preparation of gecko-inspired smart membranes

As illustrated in Fig. 2A, the fabrication of highly sensitive mechano-optical membranes involved three steps: spray coating of silica NPs onto a polystyrene substrate, spray coating of dye, as well as casting and curing of PDMS precursor. Two kinds of dyes with plane molecular structures, e.g. Disperse Blue E-4R (1,5-Diamino-2-chloro-4,8-dihydroxy-9,10-anthracenedione) and Sudan II (1-(2,4-Xylidylazo)-2-naphthol), were chosen and marked as dye(D) and dye(S), respectively. After the spray coating of dye, the dyes are uniformly coated on the surface of silica NPs and rarely filled the pores in NPs arrays (Fig. 2B and 2C). To investigate the influence of dye content in the dye coated NPs arrays (dye@NPs), dye solution was sprayed by different spray times. Calculated from the thermogravimetric curve, Fig. S1 indicated that dye content was increased by ~ 1.45 wt% for each spraying. When dye

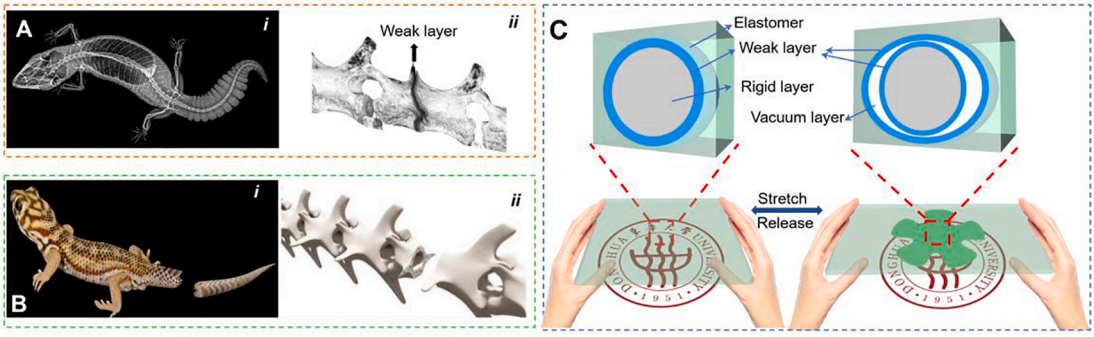

Fig. 1. Illustrations of the concept of gecko-inspired ultrasensitive mechano-optical membranes. (A) X-ray image of gecko and its caudal vertebrae. (B) Optical image for tail amputation of gecko via the weak non-ossificated septum. (C) Schematic for ulatrasensitive mechano-optical membrane based on weak layer.

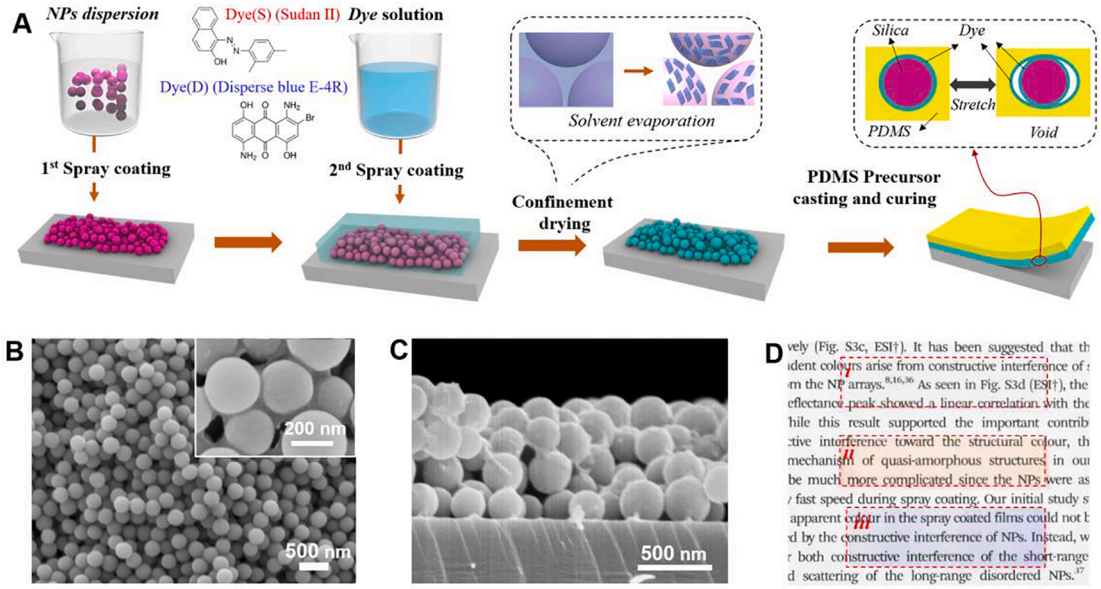

Fig. 2. Schematic for the fabrication of ultrasensitive smart membrane and their images. (A) Schematic of ultrasensitive smart membrane. (B) SEM images of dye(S)@NPs layer. (C) Cross-sectional SEM image of dye(D)@NPs layer. (D) Optical images of optical tunable membrane. *i*: NPs/PDMS; *ii*: dye(S)@NPs/PDMS; *iii*: dye(D)@NPs/PDMS.

sprayed for greater times (>6 times), it was obviously found dye filled the gaps of NPs arrays (Fig. S2). Compared to initial morphology of silica NPs arrays (Fig. S3), dye@NPs arrays with dyes of 8.5 wt% (6 times spraying) kept the uniform amorphous structure with the 3D connected porous. In contrast, there were aggregations and clogging in mixed arrays through co-spraying of dye and NPs mixture (Fig. S4). The 3D connected porous structure of dye@NPs arrays could help complete infiltration of PDMS precursor in the NPs arrays. An interfacial layer of dye was formed between NPs and PDMS (see schematic in Fig. 2A). After thermal curing of PDMS precursor, a transparent dye@NPs/PDMS composite membrane with light color was obtained (Fig. 2D).

Due to the light absorption of dye, dye@NPs/PDMS membranes had an average transmittance decrease of 8% than NPs/PDMS membranes at visible range (Fig. S5). Dye@NPs/PDMS membrane was reversibly mechano-optical responsive under stretching (see Video S1), which was similar like NPs/PDMS membrane we reported previously [24] due to the substantial scattering caused by the nanocavitation (see schematic in Fig. 2A). The transmittances of dye@NPs/PDMS membranes at varied strain were characterized to quantitatively investigate their optical tunable behavior. Firstly, it was found the mechano-optical response was highly affected by the content of dye. Fig. S6 summarized the transmittance (at wavelength of 550 nm) of dye(D)@NPs/PDMS membranes with various dye spraying times when applied strain from 0 to 100%. From the transmittance change from strain of 0 to 20% (Fig. S6B), it clearly indicated 6 times of dye spraying generated the highest transmittance loss (60%). It was mainly because critical dye content (here is 8.5 wt%) could guarantee a complete coat on the surface of NPs arrays without any pore blocking. Thus, the optimum dye spraying cycle

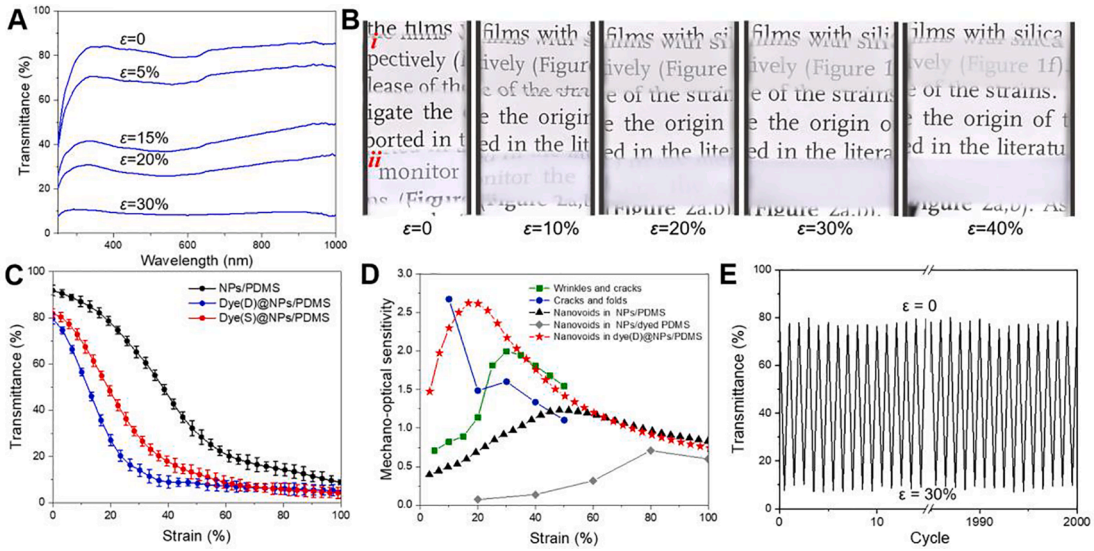

Fig. 3. Senstivity of smart membranes. (A) Transmittance spectra of dye(D)@NPs/PDMS membranes upon stretching. (B) Optical images of smart membranes without (*i*) or with (*ii*) dye layer. (C) Transmittance at wavelength of 550 nm of different tunable membranes as a function of applied strain. (D) Comparison of mechanical-optical sensitivity between our work and other reported results from similar mechano-optical tunable materials. (E) Transmittance at wavelength of 550 nm versus stretching/release cycle numbers.

of 6 times was chosen for the following fabrication.

3.2. Sensitivity of gecko-inspired mechano-optical membranes

Fig. 3A listed the transmittance changes upon stretching of dye(D)@NPs/PDMS membranes. Importantly, the transmittance could be dropped at small strain. Fig. 3B, Fig. S7 and Fig. S8 also demonstrated the optical images and transmittance changes at 550 nm upon stretching. As summarized in Fig. 3C, the transmittance at 550 nm of dye(D)@NPs/PDMS could be dramatically reduced by ~44% and ~70% at small strain 15% and 30%, respectively. While the transmittance of dye(S)@NPs/PDMS could be reduced by ~38% and ~57% at strain 15% and 30%, respectively. In contrast, NPs/PDMS membrane only showed transmittance loss of 15% and 30% at strain 15% and 30%, respectively. The drastically change of transmittance at small strain scale was very important for the practical applications in smart windows and mechanical sensors taking into the account the running cost.

To quantitatively analyze the strain sensitivity of mechano-optical membranes, based on similar definition of gauge factor from electrical resistance [30,31] and light intensity [32], we define the mechano-optical sensitivity (S) as follows:

$$S = \left|\frac{T_\varepsilon - T_0}{\varepsilon}\right| \quad (1)$$

where ε is the strain, T_0 and T_ε are the transmittance (wavelength of 550 nm) at initial state ($\varepsilon = 0$) and stretching at a certain strain (ε), respectively. According to the definition of sensitivity, the curves of sensitivity *vs* strain of dye(D)@NPs/PDMS, dye(S)@NPs/PDMS and NPs/PDMS were plotted in Fig. S9. It indicated utilizing dye as the interfacial layer between NPs and PDMS, the highest mechano-optical sensitivity could be improved to 2.62 from 1.23 of NPs/PDMS. Moreover, we compared with other reported strain-induced optical tunable materials based on dynamic surface patterns, e.g. cracks/folds [21,22], wrinkling-cracking [23] and formation/vanishment of nanovoids in NP-embedded composites [24,25] (Fig. 3D and Table S1). It clearly demonstrates that the sensitivity in our work is extremely high and very closed to the highest sensitivity of cracks/folds system ($S = 2.67$ at 10%) [21,22], while the sensitivities of other reported mechano-optical membranes changed from transparent to opaque (D) or from opaque to transparent (Fig. S10) are almost lower than 2. It is also found dye(D)@NPs/PDMS has an abroad range of high sensitivity ($S > 2$) from $\varepsilon = 7\%$ to $\varepsilon = 33\%$, which indicates the continued fast decrease of transparency when stretching. The normal transmittance at 550 nm versus release/stretching cycles are exhibited in Fig. 3E. Even after 2000 cycles, the transmittance curves at release or stretching state show negligible difference from that at initial release state or after first stretching. This result indicates the excellent robustness of our optical tunable membranes.

3.3. Mechanism for the ultrasensitivity of smart membranes

To furtherly investigate the influence of dyes on the interface interaction between silica NPs and PDMS, experimental peeling force tests, void generation monitoring and theoretical molecular dynamics simulation were carried out. The peeling force of quartz slide/PDMS membrane and dye coated quartz slide/PDMS membrane were measured by 90° peeling test (see details in supporting information) [33] to approximately characterize the interface energy between silica NPs and PDMS. Fig. 4A exhibits that the introduction of dyes can greatly reduce the peeling force between quartz slide and PDMS membrane, which confirms the presence of dye-induced weak-boundary layer. More, larger silica beads (diameter of ~100 μm) were used to better observe the void generation of composite membranes upon stretching. Fig. 4B shows the optical microscope photos of composite membrane with or without dye, indicating that voids begin to form at strain of 5–6% while voids show up later at strain of 10% for dye-free composite membrane. To quantitatively describe the void generation process, here the area of optical interface (S_{opt}) is defined as the surface area of void between NPs and PDMS (see Fig. S12). In order to eliminate the effect of NPs size, the optical interface ratio (I_{opt}) is defined as the ratio of optical interface area to the surface area of NPs, which could be calculated from:

$$Iopt = \frac{2\pi Rh + \frac{2}{3}\pi(2ab + a^2)}{4\pi R^2} \quad (2)$$

The details for the calculation could be seen in support information. As shown in Fig. 4C, the optical interface area in dye-containing

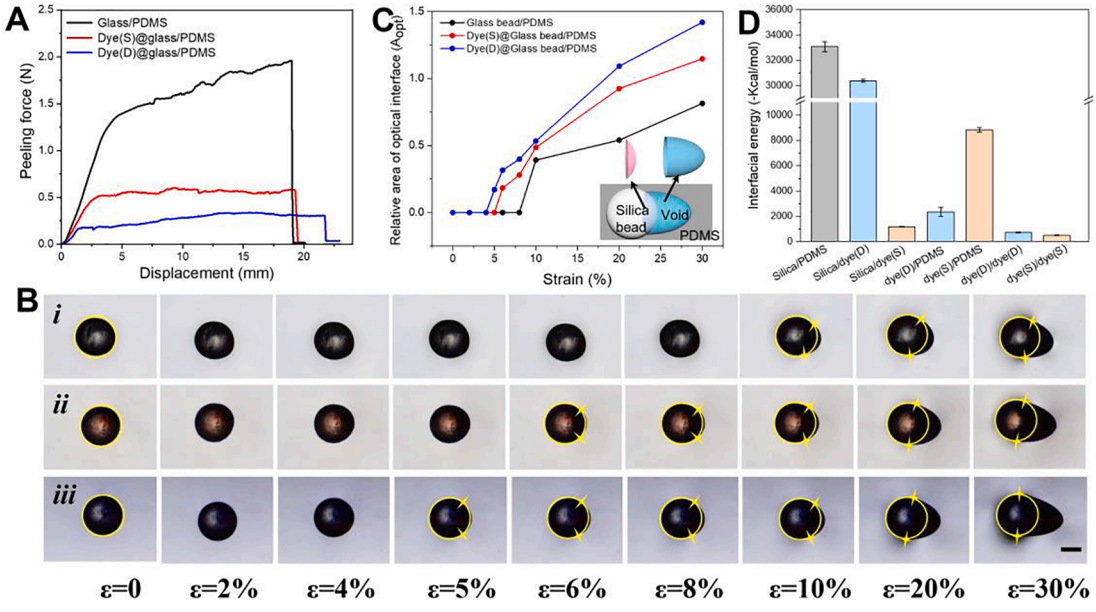

Fig. 4. Dye-induced weak interface force. (A) Peeling force of glass/PDMS (black), dye(S)@glass/PDMS (red), dye(D)@glass/PDMS (blue). (B) Optical microscope photograph at various strains of *i*): glass bead/PDMS, , *ii*): dye(S)@glass bead/PDMS, *iii*): dye(D)@glass bead/PDMS (blue) after multiple stretching. Scale bar: 50 μm. (C) Surface area of optical interface at various strains. Inset: schematic diagram of void generation. (D) Interfacial energy of various interfaces through molecular dynamics simulations.

membrane is greater than that of dye-free sample under the same condition. As a result, the transmittance loss is greatly enhanced due to the high diffusion scattering of the strain-induced optical interfaces. Additionally, molecular dynamics simulation (Fig. S13) was performed to estimate the interfacial energy. While the interfacial energy between dye/NPs, dye/dye, dye/PDMS and NPs/PDMS were calculated in Fig. 4D. Here ignoring the spatial aggregation behavior, the molecules of dye(D) and dye(S) are randomly distributed in simulation. The results indicate that the interfacial energy between dye/dye is about 1/50 of that of NPs/PDMS, while the interfacial energy of dye(D)/PDMS or dye (S)/NPs is one magnitude smaller than that of NPs/PDMS. Here PDMS and NPs are considered as soft and rigid domain, then dye is a stiff layer. It is deduced that the voids are firstly generated due to the separation of weak dye/dye interface in the NPs/PDMS composite membrane system, shown as the inset schematic in Fig. 2A. The introduction of dye stiff layer greatly enhances the formation of scattering interface, which subsequently improves the mechano-optical sensitvity. That is consistent with the above results about peeling force, optical change upon stretching. Actually, partial crystallization of dye occurs due to the plane structure and large π bond of dye molecule. Fig. S14 and Table S2 in support information summarize the crystallinity of sprayed two kinds of dyes coating and the sprayed dye on silica NPs arrays. Dye(S) has high crystallinity than dye(D), however, the crystallizations of two dyes are both highly suppressed by the NPs arrays with submicron porous. It is believed that higher crystallinity of dye(S) enhances the interfacial energy at dye(S)/dye(S) than dye(D)/dye(D), which reducing the mechano-optical sensitivity accordingly.

3.4. Potential applications of ultrasensitive smart membranes

Based on the ultra-high sensitivity of optical tuning upon facile stretching, these dye-containing composite membranes could be used in smart windows, display, security, sensors, etc. In order to improve the visibility and artistic value of tunable optical membranes and accordingly widen their application fields, herein colored tunable optical membrane was designed as illustrated in Fig. 5A-*i*. In the top layer, dye dispersed PDMS precursor solution was casted over the dye@NPs arrays and then cured, providing an expected color. Firstly, in order to separate the influence of two layers on transmittance tuning upon stretching, single dye dispersed PDMS membranes with different colors from different dyes were fabricated and their transmittance were investigated. The optical images and transmittance at wavelength of 550 nm (Fig. S16) demonstrate that the transmittance seems unchanged upon stretching 0–100% strain. Theoretically, the transmittance of dye dispersed PDMS layer during one directional stretching could be calculated by Beer-Lambert law [34]:Fig. 6.

$$T\varepsilon = T_0^{\frac{1}{(1+\varepsilon_x)(1-\nu\varepsilon_x)}} \quad (3)$$

where T_ε is transmittance under strain, T_0 is the initial transmittance, ε_x is the strain in the direction of tension, $\nu = 0.46$ is Poisson ratio. The detailed calculation could be found in support information. Both the simulation (Fig. 5A-*ii*) and experimental results (Fig. S17) showed that the addition of dyes in the top layer totally couldn't change the transmittance tuning of composite membrane. From this design of colored tunable optical membranes, colored smart membranes dye(D)@NPs/dye(D) dispersed PDMS was fabricated. As illustrated in Fig. 5C and Fig. S17, the colored smart membrane also shows high mechano-optical sensitivity (S = 2.62 at a strain of 20%) and great optical tuning range (~67%). Fig. 5D demonstrates the promising application of various colored smart membranes in smart window.

Moreover, we also demonstrate the colored smart membranes can be applied in sensors and anti-counterfeiting. First, it could be used as the healthcare sensor for robots (Fig. 6AA) or human bodies, e.g. visible medical bandages. Utilizing the scattering mechanism of the highly sensitive smart membranes, Fig. 6B shows the optical transmittance change while stretching. In order to improve the contrast between the body and smart membrane, carbon nanotubes (CNTs) dispersed PDMS was used as the background layer. Fig. 6C shows the color change of the smart membrane when bending the wooden finger clearly. By using dye-coated or dye-free NPs locally, the robust smart membranes could exhibit different sensitivity in different areas (Fig. 6D). Upon mechanical stretching, the smart membrane shows different transmittances in different areas, making the smart membranes candidate for anti-counterfeiting (Video S3). As illustrated in Fig. 6E, a pattern of a dolphin with a ball was embedded in the composite films by a mask during spraying. This pattern could be reversibly revealed upon stretching and releasing.

4. Conclusions

Inspired from the fast tail amputation of gecko, here we

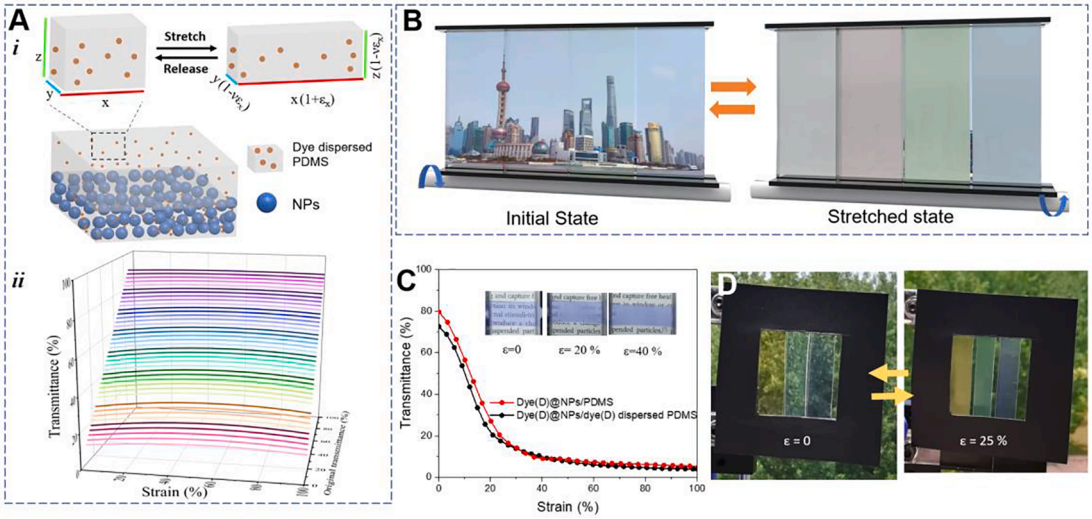

Fig. 5. Schematic illustration and images for the application as ultrasensitive colored smart window. (A) Schematic for the design of two-layered colored optical tunable membranes (*i*) and calculated transmittance spectra of top dye dispersed PDMS layer as a functional of stretching strain and dye concentration. (B) Schematic illustration for the colored smart window. (C) Transmittance at wavelength of 550 nm versus strain of dye(D)@NPs/dye(D) dispersed PDMS. Inset: its optical images at strain of 0, 20% and 40%. (D) Photographs of colored smart window at applied strains of 0 and 25%.

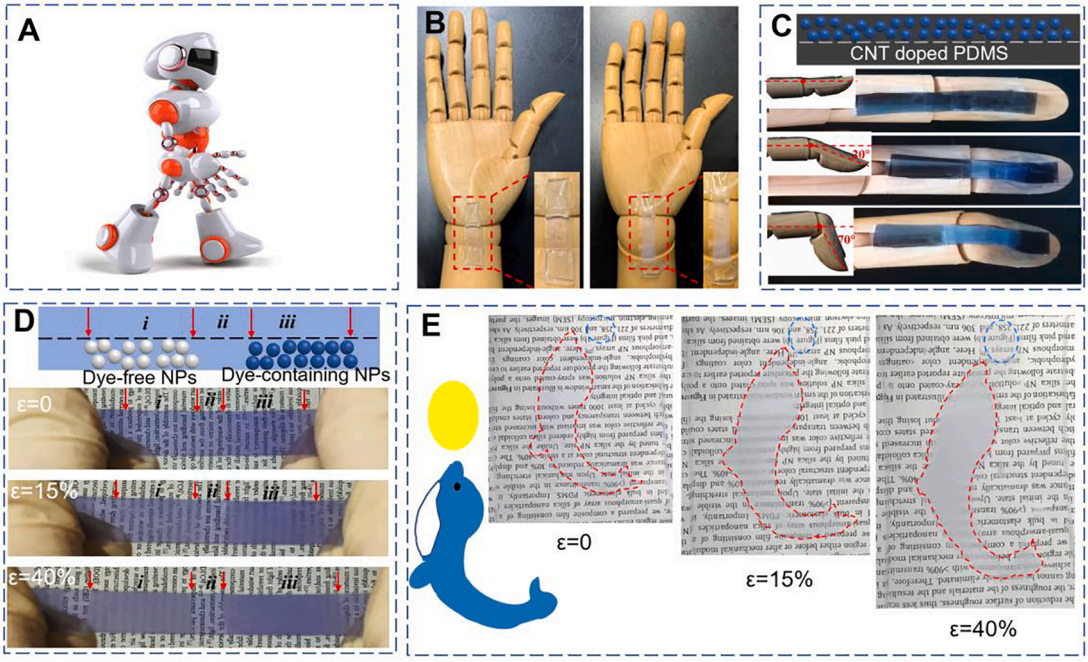

Fig. 6. Schematic illustration and images for applications in sensors and anti-counterfeiting. (A) Image of a robot, and optical images of (B) elbow smart skin and (C) colored smart finger sensor based on our smart membrane. (D) Schematic and optical images of smart membrane which can reversibly display and hide information upon stretching. (E) Tunable dolphin pattern with stretching for anti-counterfeiting.

demonstrated an ultrasensitive multifunctional mechano-optical sensor. The optical transmittance of the smart membrane can be linearly reduced by 44% upon stretching to 15% strain. Additionally, high sensitivity ($S > 2$) is displayed within an abroad range from $\varepsilon = 7\%$ to $\varepsilon = 33\%$. This ultrasensitive smart membrane has a total tuning range of 75% and shows high robustness in repeated stretching and releasing (at least 2000 cycles). The dye-induced weak-boundary layer is confirmed by the experimental results and interfacial energy simulation. We also design colored ultrasensitive smart membrane and demonstrate their applications in smart window, anti-counterfeiting, sensors. It is believed that we provide a facile, low-cost approach to develop robust and highly sensitive mechano-optical device. Further, this interface design can be extended to other smart mechano-responsive materials for fabrication of ultrasensitive device via deformation under external stimuli such as force, heat, light, moisture, solvent.

Declaration of Competing Interest

The authors declare that they have no known competing financial interests or personal relationships that could have appeared to influence the work reported in this paper.

Acknowledgements

This work is supported by the National Natural Science Foundation of China 11774049 and 51973033, and the Fundamental Research Funds for the Central Universities 2232021D-02.

Appendix A. Supplementary data

Supplementary data to this article can be found online at https://doi.org/10.1016/j.cej.2021.132159.

References

[1] Z.F. Liu, S. Fang, F.A. Moura, J.N. Ding, N. Jiang, J. Di, M. Zhang, X. Lepro, D. S. Galvao, C.S. Haines, N.Y. Yuan, S.G. Yin, D.W. Lee, R. Wang, H.Y. Wang, W. Lv, C. Dong, R.C. Zhang, M.J. Chen, Q. Yin, Y.T. Chong, R. Zhang, X. Wang, M.D. Lima, R. Ovalle-Robles, D. Qian, H. Lu, R.H. Baughman, Hierarchically buckled sheath-core fibers for superelastic electronics, sensors, and muscles, Science 349 (6246) (2015) 400–404.
[2] X. Feng, G. Zhang, B.o. Xu, H. Jiang, Q. Bai, H. Li, Self-healing elastomer assembly towards three-dimensional shape memory devices, RSC Adv. 5 (86) (2015) 70000–70004.
[3] H.X. Zhao, Q.Q. Sun, J. Zhou, X. Deng, J.X. Cui, Switchable cavitation in silicone coatings for energy-saving cooling and heating, Adv. Mater. 32 (2020) 2000870.
[4] R. Vergaz, J.-M. Sánchez-Pena, D. Barrios, C. Vázquez, P. Contreras-Lallana, Modelling and electro-optical testing of suspended particle devices, Sol. Energy Mater. Sol. Cells 92 (11) (2008) 1483–1487.
[5] D. Cupelli, F. Pasquale Nicoletta, S. Manfredi, M. Vivacqua, P. Formoso, G. De Filpo, G. Chidichimo, Self-adjusting smart windows based on polymer-dispersed liquid crystals, Sol. Energy Mater. Sol. Cells 93 (11) (2009) 2008–2012.
[6] S.-M. Guo, X. Liang, C.-H. Zhang, M. Chen, C. Shen, L.-Y. Zhang, X. Yuan, B.-F. He, H. Yang, Preparation of a thermally light-transmittance-controllable film from a coexistent system of polymer-dispersed and polymer-stabilized liquid crystals, ACS Appl. Mater. Interfaces 9 (3) (2017) 2942–2947.
[7] C.D. Sheraw, L. Zhou, J.R. Huang, D.J. Gundlach, T.N. Jackson, M.G. Kane, I. G. Hill, M.S. Hammond, J. Campi, B.K. Greening, J. Francl, J. West, Organic thin-film transistor-driven polymer-dispersed liquid crystal displays on flexible polymeric substrates, Appl. Phys. Lett. 80 (6) (2002) 1088–1090.
[8] C. Bechinger, S. Ferrere, A. Zaban, J. Sprague, B.A. Gregg, Photoelectrochromic windows and displays, Nature 383 (6601) (1996) 608–610.
[9] I.P. Parkin, T.D. Manning, Intelligent thermochromic windows, J. Chem. Educ. 83 (3) (2006) 393–400.
[10] C.G. Granqvist, P.C. Lansåker, N.R. Mlyuka, G.A. Niklasson, E. Avendaño, Progress in chromogenics: New results for electrochromic and thermochromic materials and devices, Sol. Energy Mater. Sol. Cells 93 (12) (2009) 2032–2039.
[11] C.M. Lampert, Chromogenic smart materials, Mater. Today 7 (3) (2004) 28–35.
[12] H.N. Apostoleris, M. Chiesa, M. Stefancich, Improved transparency switching in paraffin-PDMS composites, J. Mater. Chem. C 3 (6) (2015) 1371–1377.
[13] H. Apostoleris, M. Stefancich, S. Lilliu, M. Chiesa, Sun-tracking optical element realized using thermally activated transparency-switching material, Opt. Express 23 (15) (2015) A930–A935.
[14] S.G. Lee, D.Y. Lee, H.S. Lim, D.H. Lee, S. Lee, K. Cho, Switchable transparency and wetting of elastomeric smart windows, Adv. Mater. 22 (44) (2010) 5013–5017.
[15] E. Lee, M. Zhang, Y. Cho, Y. Cui, J. Van der Spiegel, N. Engheta, S. Yang, Tilted pillars on wrinkled elastomers as a reversibly tunable optical window, Adv. Mater. 26 (24) (2014) 4127–4133.
[16] H. Lee, J.G. Bae, W.B. Lee, H. Yoon, Mechano-responsive lateral buckling of miniaturized beams standing on flexible substrates, Soft Matter 13 (45) (2017) 8357–8361.
[17] J. Yang, H. Lee, S.G. Heo, S. Kang, H. Lee, C.H. Lee, H. Yoon, Squid-inspired smart window by movement of magnetic nanoparticles in asymmetric confinement, Adv. Mater. Technol. 4 (2019) 1900140.

[18] H. Xu, C. Yu, S. Wang, V. Malyarchuk, T. Xie, J.A. Rogers, Deformable, programmable, and shape-memorizing micro-optics, Adv. Funct. Mater. 23 (26) (2013) 3299–3306.
[19] J. Li, J. Shim, J. Deng, J.T.B. Overvelde, X. Zhu, K. Bertoldi, S. Yang, Switching periodic membranes via pattern transformation and shape memory effect, Soft Matter 8 (40) (2012) 10322–10328.
[20] G. Lin, P. Chandrasekaran, C. Lv, Q. Zhang, Y. Tang, L. Han, J. Yin, Self-similar hierarchical wrinkles as a potential multifunctional smart window with simultaneously tunable transparency, structural color, and droplet transport, ACS Appl. Mater. Interfaces 9 (31) (2017) 26510–26517.
[21] S.S. Zeng, D.Y. Zhang, W.H. Huang, Z.F. Wang, S.G. Freire, X.Y. Yu, A.T. Smith, E. Y. Huang, H. Nguon, L.Y. Sun, Bio-inspired sensitive and reversible mechanochromisms via strain-dependent cracks and folds, Nat. Commun. 7 (2016) 11802.
[22] Z. Mao, S. Zeng, K. Shen, A.P. Chooi, A.T. Smith, M.D. Jones, Y. Zhou, X. Liu, L. Sun, Dynamic mechanochromic optics with tunable strain sensitivity for strain-responsive digit display, Adv. Opt. Mater. 8 (2020) 2001472.
[23] Z.W. Li, Y. Zhai, Y. Wang, G.M. Wendland, X.B. Yin, J.L. Xiao, Harnessing surface wrinkling-cracking patterns for tunable optical transmittance, Adv. Opt. Mater. 5 (2017) 1700425.
[24] D.T. Ge, E. Lee, L.L. Yang, Y.G. Cho, M. Li, D.S. Gianola, S. Yang, A robust smart window: reversibly switching from high transparency to angle-independent structural color display, Adv. Mater. 27 (2015) 2489–2495.
[25] H.N. Kim, D.T. Ge, E. Lee, S. Yang, Multistate and on-demand smart windows, Adv. Mater. 30 (2018) 1803847.
[26] Y.J. Jiang, S.S. Zeng, Y. Yao, S.Y. Xu, Q.N. Dong, P.X. Chen, Z.F. Wang, M. Zhang, M.T. Zhu, G.F. Xu, H.D. Zeng, L.Y. Sun, Dynamic optics with transparency and color changes under ambient conditions, Polymers 11 (2019) 103.
[27] E.A.B. Gilbert, S.L. Payne, M.K. Vickaryous, The anatomy and histology of caudal autotomy and regeneration in lizards, Physiol. Biochem. Zool. 86 (6) (2013) 631–644.
[28] Y. Song, D.L. Villeneuve, K. Toyota, T. Iguchi, K.E. Tollefsen, Ecdysone receptor agonism leading to lethal molting disruption in arthropods: review and adverse outcome pathway development, Environ. Sci. Technol. 51 (2017) 4142–4157.
[29] D. Coates, Polymer-dispersed liquid crystals, J. Mater. Chem. 5 (12) (1995) 2063–2072.
[30] J.-Y. Jeon, T.-J. Ha, Waterproof electronic-bandage with tunable sensitivity for wearable strain sensors, ACS Appl. Mater. Interfaces 8 (4) (2016) 2866–2871.
[31] L. Lin, S. Liu, Q.i. Zhang, X. Li, M. Ji, H. Deng, Q. Fu, Towards tunable sensitivity of electrical property to strain for conductive polymer composites based on thermoplastic elastomer, ACS Appl. Mater. Interfaces 5 (12) (2013) 5815–5824.
[32] J. Gu, D. Kwon, J. Ahn, I. Park, Wearable strain sensors using light transmittance change of carbon nanotube-embedded elastomers with microcracks, ACS Appl. Mater. Interfaces 12 (9) (2020) 10908–10917.
[33] S.C. Park, S.S. Yoon, J.D. Nam, Surface characteristics and adhesive strengths of metal on O2 ion beam treated polyimide substrate, Thin Solid Films 516 (10) (2008) 3028–3035.
[34] F. López Jiménez, S. Kumar, P.M. Reis, Soft color composites with tunable optical transmittance, Adv. Opt. Mater. 4 (4) (2016) 620–626.